

**Prompt  $J/\psi$  production at the LHC: New evidence for the  $k_T$  factorization**S. P. Baranov,<sup>1</sup> A. V. Lipatov,<sup>2</sup> and N. P. Zotov<sup>2</sup><sup>1</sup>*P. N. Lebedev Physics Institute, 119991 Moscow, Russia*<sup>2</sup>*Skobeltsyn Institute of Nuclear Physics, M. V. Lomonosov Moscow State University, 119991 Moscow, Russia*

(Received 19 August 2011; published 27 January 2012)

In the framework of the  $k_T$ -factorization approach, the production and polarization of prompt  $J/\psi$  mesons in  $pp$  collisions at the LHC energy  $\sqrt{s} = 7$  TeV is studied. Both the direct production mechanism as well as feed-down contributions from  $\chi_{c1}$ ,  $\chi_{c2}$ , and  $\psi'$  decays are taken into account. Our consideration is based on the color singlet model supplemented with the off-shell matrix elements for the corresponding partonic subprocesses. The unintegrated gluon densities in a proton are determined using the CCFM evolution equation as well the Kimber-Martin-Ryskin prescription. We compare our numerical predictions with the first experimental data taken by the CMS, ATLAS, and LHCb collaborations. The estimation of polarization parameters  $\lambda_\theta$ ,  $\lambda_\phi$ , and  $\lambda_{\theta\phi}$  which determine  $J/\psi$  spin density matrix is performed.

DOI: 10.1103/PhysRevD.85.014034

PACS numbers: 12.38.-t, 13.20.Gd, 13.88.+e

**I. INTRODUCTION**

The production of charmonium states at high energies is under intense theoretical and experimental study [1–3]. The puzzling history traces back to the early 1990s, when the measurements of the  $J/\psi$  and  $\Upsilon$  hadroproduction cross sections at Tevatron energies revealed a more than one order-of-magnitude discrepancy with the theoretical expectations of the color singlet (CS) model [4]. This fact has induced extensive theoretical activity, mainly in the description of the formation of bound  $q\bar{q}$  state from the heavy quark pair produced in the hard interaction (photon-gluon or gluon-gluon fusion). In the CS model, only those states with the same quantum numbers as the resulting charmonium contribute to the formation of a bound state. In the color octet (CO) model [5], it was suggested to add the contribution of transition mechanism from  $c\bar{c}$  pairs to charmonium, where a charmed quark pair is produced in CO states ( $^1S_0^{[8]}$ ,  $^3S_1^{[8]}$ ,  $^3P_J^{[8]}$ ) and transforms into the final physical quarkonia by the help of nonperturbative soft gluon radiation. The CO model is based on the general principle of the nonrelativistic QCD factorization (NRQCD) [6]. As is well-known, the sole leading order (LO) CS model is insufficient to describe the experimental data on the  $J/\psi$  production at the Tevatron energies. By adding the contribution from the CO and fitting the free parameters one was able to describe the data on the  $J/\psi$  production at energies of modern colliders (see [7] and references therein). But to achieve agreement between the last calculations and the experimental data for the  $p_T$ -distributions measured at HERA and Tevatron the contribution of CO P-wave  $^3P_J^{[8]}$  state to be assumed is negative [8,9] in the specific region of phase-space.<sup>1</sup>

<sup>1</sup>The sole  $^3P_J^{[8]}$  contribution depends on the choice of the NRQCD factorization scheme.

However, recently the next-to-leading order (NLO) [10] and dominant next-to-next-to-leading order (NNLO\*) [11] corrections to the CS mechanism have been calculated and have been found to be essential in description of quarkonia production. The comparison with the first LHC measurements performed by the ATLAS, CMS, and LHCb collaborations demonstrates [12] that the NNLO\* CS model correctly reproduces the transverse momentum distributions as well as the total cross section of  $J/\psi$  mesons at  $\sqrt{s} = 7$  TeV.

The effect of high-order QCD corrections is also manifest in the polarization predictions. While the charmonium produced inclusively or in association with a photon are predicted to be transversely polarised at LO, it has been found that their polarization at NLO is increasingly longitudinal at high  $p_T$  [11,12]. Opposite, the LO NRQCD predicts the strong transverse polarization of the final-state quarkonia [1]. This is in disagreement with the polarization measurement [13] performed by the CDF collaboration at the Tevatron. In order to obtain the unpolarized  $J/\psi$  mesons it is necessary to assume that  $J/\psi$  production is dominated by the  $^1S_0^{[8]}$  channel [9].

The results of studies [10–12,14] support the predictions [15–24] obtained in the framework of the  $k_T$ -factorization QCD approach [25], where investigations of heavy quarkonia production and polarization have own long story. Shortly, it was demonstrated [16–23] that the experimental data on quarkonia production at HERA, RHIC and Tevatron can be well described within the CS model alone. The values of CO contributions obtained by fitting the Tevatron data appear to be substantially smaller than the ones in the NRQCD formalism [16,18,26]. Furthermore, the longitudinal polarization of produced  $J/\psi$  mesons predicted by the  $k_T$ -factorization is an immediate consequence of initial gluon off-shellness [16] which taken into account in the  $k_T$ -factorization approach.

In this paper we give the systematic analysis<sup>2</sup> of first experimental data [27–29] on the prompt  $J/\psi$  production taken by the CMS, ATLAS, and LHCb collaborations at the LHC energy  $\sqrt{s} = 7$  TeV. Following the guideline of previous studies [21,22], in our consideration we will apply the CS model supplemented with the  $k_T$ -factorization approach. Two sources of  $J/\psi$  production are taken into account: direct  $J/\psi$  production and feed-down  $J/\psi$  from the decay of other heavier prompt charmonium states like  $\chi_{c1}$ ,  $\chi_{c2}$ , or  $\psi'$ , that is in a full agreement with the experimental setup [27–29]. Specifically, we concentrate on the  $J/\psi$  spin alignment and estimate three polarization parameters  $\lambda_\theta$ ,  $\lambda_\phi$ , and  $\lambda_{\theta\phi}$  defining the spin density matrix of produced  $J/\psi$  mesons. As was mentioned above, studies of polarization observables are useful in discriminating the CS and CO production mechanisms,

The outline of our paper is following. In Sec. 2, we recall shortly the basic formulas of the  $k_T$ -factorization approach with a brief review of calculation steps. In Sec. III, we present the numerical results of our calculations and a discussion. Section IV contains our conclusions.

## II. THEORETICAL FRAMEWORK

The production of prompt  $J/\psi$  mesons in  $pp$  collisions at the LHC can proceed via either direct gluon-gluon fusion or the production of heavier  $P$ -wave states  $\chi_{cJ}$  ( $J = 0, 1, 2$ ) and  $S$ -wave state  $\psi'$ , followed by their radiative decays  $\chi_{cJ} \rightarrow J/\psi + \gamma$  and  $\psi' \rightarrow J/\psi + X$ . In the CS model, the direct mechanism corresponds to the partonic subprocess  $g^* + g^* \rightarrow J/\psi + g$  which includes the emission of an additional hard gluon in the final state. The production of  $P$ -wave quarkonia is given by  $g^* + g^* \rightarrow \chi_{cJ}$  [23] and there is no emission of any additional gluons. The feed-down contribution from the  $S$ -wave state  $\psi'$  is described by the  $g^* + g^* \rightarrow \psi' + g$  subprocess. Note that the next-to-leading-order process  $g^* + g^* \rightarrow \chi_{cJ} + g$  is expected to be much less important. Apart from one extra power of  $\alpha_s$ , it is suppressed by the relatively large invariant mass of the two-body final state, as compared to a relatively low single-body mass  $m_{\chi_{cJ}}$ . This is exactly the same reason that makes the direct  $g^* + g^* \rightarrow J/\psi + g$  and feed-down  $g^* + g^* \rightarrow \chi_{cJ} \rightarrow J/\psi + \gamma$  contributions comparable in size, despite the latter is suppressed by the  $P$ -state wave function and  $\chi_{cJ}$  decay branchings. Because of the relatively higher final-state mass, the two-body processes are much less favorable than the single-body ones. It is also worth mentioning that the only diagram contributing to the  $g^* + g^* \rightarrow \chi_c + g$  process at large  $p_T$  is the one containing three-gluon coupling and  $t$ -channel gluon propagator. This diagram is efficiently present in our calculations. In fact, it can be considered as the lowest-order  $g^* + g^* \rightarrow \chi_c$  subprocess combined with initial-state gluon radiation. The latter is taken into

account in the form of the evolution of gluon densities. This illustrates the advantage of the  $k_T$ -factorization approach that gives access to the effects of NLO contributions even with the formally LO matrix elements for the hard partonic subprocess. So, to avoid double counting, the NLO  $g^* + g^* \rightarrow \chi_c + g$  subprocess should be omitted from our analysis.

The production amplitudes of the subprocesses above can be obtained from the one for an unspecified  $c\bar{c}$  state by the application of appropriate projection operators  $J(S, L)$  which guarantee the proper quantum numbers of the  $c\bar{c}$  state under consideration. These operators for the spin triplet states can be written as [4]

$$J(^3S_1) = \hat{\epsilon}(S_z)(\hat{p}_c + m_c)/m^{1/2}, \quad (1)$$

$$J(^3P_J) = (\hat{p}_{\bar{c}} - m_c)\hat{\epsilon}(S_z)(\hat{p}_c + m_c)/m^{3/2}, \quad (2)$$

where  $m$  is the mass of the specifically considered  $c\bar{c}$  state,  $p_c$  and  $p_{\bar{c}}$  are the four-momenta of the charmed quark and antiquark. In accordance with the nonrelativistic formalism of bound state formation, the charmed quark mass  $m_c$  is always set equal to 1/2 of the quarkonium mass. States with various projections of the spin momentum onto the  $z$  axis are represented by the polarization vector  $\epsilon(S_z)$ .

The probability for the two quarks to form a meson depends on the bound state wave function  $\Psi(q)$ . In the nonrelativistic approximation, the relative momentum  $q$  of the quarks in the bound state is treated as a small quantity. So, we represent the quark momenta as follows:

$$p_c = p/2 + q, \quad p_{\bar{c}} = p/2 - q, \quad (3)$$

where  $p$  is the four-momentum of the final state quarkonium. Then, we multiply the relevant partonic amplitude  $\mathcal{A}$  (depending on  $q$ ) by  $\Psi(q)$  and perform integration with respect to  $q$ . The integration is performed after expanding the integrand around  $q = 0$ :

$$\mathcal{A}(q) = \mathcal{A}|_{q=0} + q^\alpha(\partial\mathcal{A}/\partial q^\alpha)|_{q=0} + \dots \quad (4)$$

The first term in (4) corresponds to  $L = 0$  state and the second one to  $L = 1$ . Since the expressions for  $\mathcal{A}|_{q=0}$  and  $\partial\mathcal{A}/\partial q^\alpha|_{q=0}$  are no longer dependent on  $q$ , they may be factored outside the integral sign. A term-by-term integration of this series then yields [30]

$$\int \frac{d^3q}{(2\pi)^3} \Psi(q) = \frac{1}{\sqrt{4\pi}} \mathcal{R}(x=0), \quad (5)$$

$$\int \frac{d^3q}{(2\pi)^3} q^\alpha \Psi(q) = -i\epsilon^\alpha(L_z) \frac{\sqrt{3}}{\sqrt{4\pi}} \mathcal{R}'(x=0), \quad (6)$$

where  $\mathcal{R}(x)$  is the radial wave function in the coordinate representation, i.e. the Fourier transform of  $\Psi(q)$ . The first term in (4) contributes only to  $S$  waves, but vanishes for  $P$  waves because  $\mathcal{R}_P(0) = 0$ . On the contrary, the second term contributes only to  $P$  waves, but vanishes for  $S$  waves

<sup>2</sup>See also [24].

because  $\mathcal{R}'_S(0) = 0$ . States with various projections of the orbital angular momentum onto the  $z$  axis are represented by the polarization vector  $\epsilon(L_z)$ . The numerical values of the wave functions are either known from the leptonic decay widths (for  $J/\psi$  and  $\psi'$  mesons) or can be taken from potential models (for  $\chi_{cJ}$  mesons).

In our numerical calculations, the polarization vectors  $\epsilon(S_z)$  and  $\epsilon(L_z)$  are defined as explicit four-vectors. In the frame where the  $z$  axis is oriented along the quarkonium momentum vector  $p^\mu = (E, 0, 0, |\mathbf{p}|)$ , these polarization vectors read

$$\epsilon^\mu(\pm 1) = (0, \pm 1, i, 0)/\sqrt{2}, \quad \epsilon^\mu(0) = (|\mathbf{p}|, 0, 0, E)/m. \quad (7)$$

The states with definite  $S_z$  and  $L_z$  are translated into states with definite total momentum  $J$  and its projection  $J_z$  using the Clebsch-Gordan coefficients:

$$\epsilon^{\mu\nu}(J, J_z) = \sum_{S_z, L_z} \langle 1, L_z; 1, S_z | J, J_z \rangle \epsilon^\mu(S_z) \epsilon^\nu(L_z). \quad (8)$$

Further evaluation of all partonic amplitudes under consideration (including subsequent leptonic and/or radiative decays, of course) is straightforward and was done using the algebraic manipulation systems FORM [31]. We do not list here the obvious expressions because of lack of space, but only mention several technical points. First, in according to the  $k_T$ -factorization prescription [25], the summation over the incoming off-shell gluon polarizations is carried with  $\overline{\epsilon^\mu \epsilon^{*\nu}} = \mathbf{k}_T^\mu \mathbf{k}_T^\nu / \mathbf{k}_T^2$ , where  $\mathbf{k}_T$  is the gluon transverse momentum orthogonal to the beam axis. In the collinear limit, when  $|\mathbf{k}_T| \rightarrow 0$ , this expression converges to the ordinary  $\overline{\epsilon^\mu \epsilon^{*\nu}} = -g^{\mu\nu}/2$  after averaging over the azimuthal angle. In all other respects the evaluation follows the standard QCD Feynman rules. Second, the spin density matrix of final  $J/\psi$  meson is determined by the momenta  $l_1$  and  $l_2$  of the decay leptons and is taken in the form

$$\sum \epsilon^\mu \epsilon^{*\nu} = 3 \left( l_1^\mu l_2^\nu + l_1^\nu l_2^\mu - \frac{m^2}{2} g^{\mu\nu} \right) / m^2. \quad (9)$$

This expression is equivalent to the standard one  $\sum \epsilon^\mu \epsilon^{*\nu} = -g^{\mu\nu} + p^\mu p^\nu / m^2$  but is better suited for studying the polarization observables because it gives access to the kinematic variables describing the orientation of the decay plane. Third, when considering the polarization properties of  $J/\psi$  mesons originating from radiative decays of  $P$ -wave states, we rely upon the dominance of electric dipole  $E1$  transitions.<sup>3</sup> The corresponding invariant amplitudes can be written as [32]

$$i\mathcal{A}(\chi_{c1} \rightarrow J/\psi + \gamma) = g_1 \epsilon^{\mu\nu\alpha\beta} k_\mu \epsilon_\nu^{(\chi_{c1})} \epsilon_\alpha^{(J/\psi)} \epsilon_\beta^{(\gamma)}, \quad (10)$$

<sup>3</sup>The same approach has been applied [21] to study the  $Y$  production and polarization at the Tevatron.

$$i\mathcal{A}(\chi_{c2} \rightarrow J/\psi + \gamma) = g_2 p^\mu \epsilon_{(\chi_{c2})}^{\alpha\beta} \epsilon_\alpha^{(J/\psi)} [k_\mu \epsilon_\beta^{(\gamma)} - k_\beta \epsilon_\mu^{(\gamma)}], \quad (11)$$

where  $\epsilon_\mu^{(\chi_{c1})}$ ,  $\epsilon_\mu^{(J/\psi)}$ , and  $\epsilon_\mu^{(\gamma)}$  are the polarization vectors of a corresponding spin-one particles and  $\epsilon_{\mu\nu}^{(\chi_{c2})}$  is its counterpart for a spin-two  $\chi_{c2}$  meson,  $p$  and  $k$  are the four-momenta of the decaying quarkonium and the emitted photon, and  $\epsilon^{\mu\nu\alpha\beta}$  is the fully antisymmetric Levi-Civita tensor. The dominance of electric dipole transitions for the charmonium family is supported by the experimental data taken by the E835 Collaboration at the Tevatron [33]. Since the electromagnetic branching ratio for  $\chi_{c0} \rightarrow J/\psi + \gamma$  decay is more than an order of magnitude smaller than those for  $\chi_{c1}$  and  $\chi_{c2}$ , we neglect its contribution to  $J/\psi$  production. As the  $\psi' \rightarrow J/\psi + X$  decay matrix elements are unknown, these events were generated according to the phase space.

The cross section of  $J/\psi$  production at high energies in the  $k_T$ -factorization approach is calculated as a convolution of the off-shell partonic cross section and the unintegrated gluon distributions in a proton. The contribution from the direct production mechanism can be presented in the following form:

$$\begin{aligned} \sigma(pp \rightarrow J/\psi + X) &= \int \frac{1}{16\pi(x_1 x_2 s)^2} f_g(x_1, \mathbf{k}_{1T}^2, \mu^2) f_g(x_2, \mathbf{k}_{2T}^2, \mu^2) \\ &\quad \times |\overline{\mathcal{M}}(g^* + g^* \rightarrow J/\psi + g)|^2 d\mathbf{p}_T^2 d\mathbf{k}_{1T}^2 d\mathbf{k}_{2T}^2 dy dy_g \frac{d\phi_1}{2\pi} \frac{d\phi_2}{2\pi}, \end{aligned} \quad (12)$$

where  $f_g(x, \mathbf{k}_T^2, \mu^2)$  is the unintegrated gluon density,  $\mathbf{p}_T$  and  $y$  are the transverse momentum and rapidity of produced  $J/\psi$  meson,  $y_g$  is the rapidity of outgoing gluon, and  $s$  is the  $pp$  center-of-mass energy. The initial off-shell gluons have a fraction  $x_1$  and  $x_2$  of the parent protons longitudinal momenta, nonzero transverse momenta  $\mathbf{k}_{1T}$  and  $\mathbf{k}_{2T}$  ( $\mathbf{k}_{1T}^2 = -k_{1T}^2 \neq 0$ ,  $\mathbf{k}_{2T}^2 = -k_{2T}^2 \neq 0$ ) and azimuthal angles  $\phi_1$  and  $\phi_2$ . For the production of  $\chi_{cJ}$  mesons via  $2 \rightarrow 1$  subprocess above we have

$$\begin{aligned} \sigma(pp \rightarrow \chi_{cJ} + X) &= \int \frac{\pi}{x_1 x_2 s \delta} f_g(x_1, \mathbf{k}_{1T}^2, \mu^2) f_g(x_2, \mathbf{k}_{2T}^2, \mu^2) \\ &\quad \times |\overline{\mathcal{M}}(g^* + g^* \rightarrow \chi_{cJ})|^2 d\mathbf{k}_{1T}^2 d\mathbf{k}_{2T}^2 dy \frac{d\phi_1}{2\pi} \frac{d\phi_2}{2\pi}, \end{aligned} \quad (13)$$

where the off-shell gluon flux factor is equal to  $2\delta$ , where  $\hat{s}$  is the energy of partonic subprocess.<sup>4</sup> In (12) and (13),  $|\overline{\mathcal{M}}(g^* + g^* \rightarrow J/\psi + g)|^2$  and  $|\overline{\mathcal{M}}(g^* + g^* \rightarrow \chi_{cJ})|^2$  are the corresponding off-shell matrix elements squared

<sup>4</sup>The dependence of numerical predictions on the different forms of flux factor has been studied in [20].

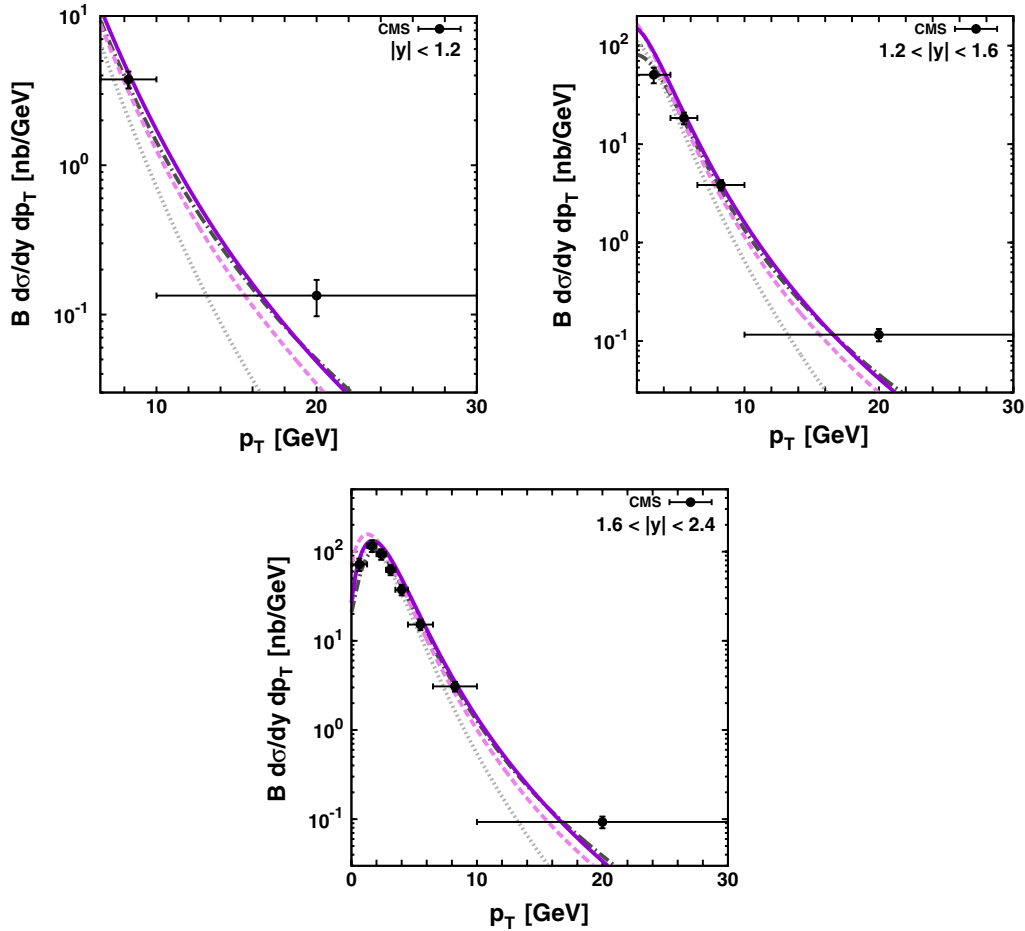


FIG. 1 (color online). The double differential cross sections  $d\sigma/dydp_T$  of prompt  $J/\psi$  production at  $\sqrt{s} = 7$  TeV compared to the CMS data [28]. The solid, dashed, and dash-dotted curves correspond to the results obtained using the CCFM A0, CCFM B0, and KMR gluon densities, respectively. The dotted curves represent the contribution from sole direct production mechanism calculated with the CCFM A0 gluon distribution.

and averaged over initial gluon polarizations and colors. The production scheme of  $\psi'$  meson is identical to that of  $J/\psi$ , and only the numerical value of the wave function  $|\mathcal{R}(0)|^2$  is different (see below).

In the numerical calculations we have tested a few different sets of unintegrated gluon distributions involved in (12) and (13). The first of them (CCFM set A0) has been obtained [34] from the CCFM equation where all input parameters have been fitted to describe the proton structure function  $F_2(x, Q^2)$ . Equally good fit of the  $F_2$  data was obtained using different values for the soft cut and a different value for the width of the intrinsic  $\mathbf{k}_T$  distribution (CCFM set B0). Also we will use the unintegrated gluons taken in the Kimber-Martin-Ryskin (KMR) form [35]. The KMR approach is a formalism to construct the unintegrated parton distributions from well-known conventional ones. For the input, we have used recent leading-order Martin-Stirling-Thorn-Watt (MSTW) set [36].

The multidimensional integrations in (12) and (13) have been performed by the means of Monte Carlo technique,

using the routine VEGAS [37]. The full C++ code is available from the author on request.<sup>5</sup>

### III. NUMERICAL RESULTS

We now are in a position to present our numerical results. First we describe our input and the kinematic conditions. After we fixed the unintegrated gluon distributions, the cross sections (12) and (13) depend on the renormalization and factorization scales  $\mu_R$  and  $\mu_F$ . Numerically, we set  $\mu_R^2 = m^2 + \mathbf{p}_T^2$  and  $\mu_F^2 = \hat{s} + \mathbf{Q}_T^2$ , where  $\mathbf{Q}_T$  is the transverse momentum of initial off-shell gluon pair. Note that the choice of  $\mu_R$  is the standard one for studying of the  $J/\psi$  production whereas the special choice of  $\mu_F$  is connected with the CCFM evolution (see [34]). Following to [38], we set  $m_{J/\psi} = 3.097$  GeV,  $m_{\chi_{c1}} = 3.511$  GeV,  $m_{\chi_{c2}} = 3.556$  GeV,  $m_{\psi'} = 3.686$  GeV and use the LO formula for the coupling constant  $\alpha_s(\mu^2)$

<sup>5</sup>lipatov@theory.sinp.msu.ru



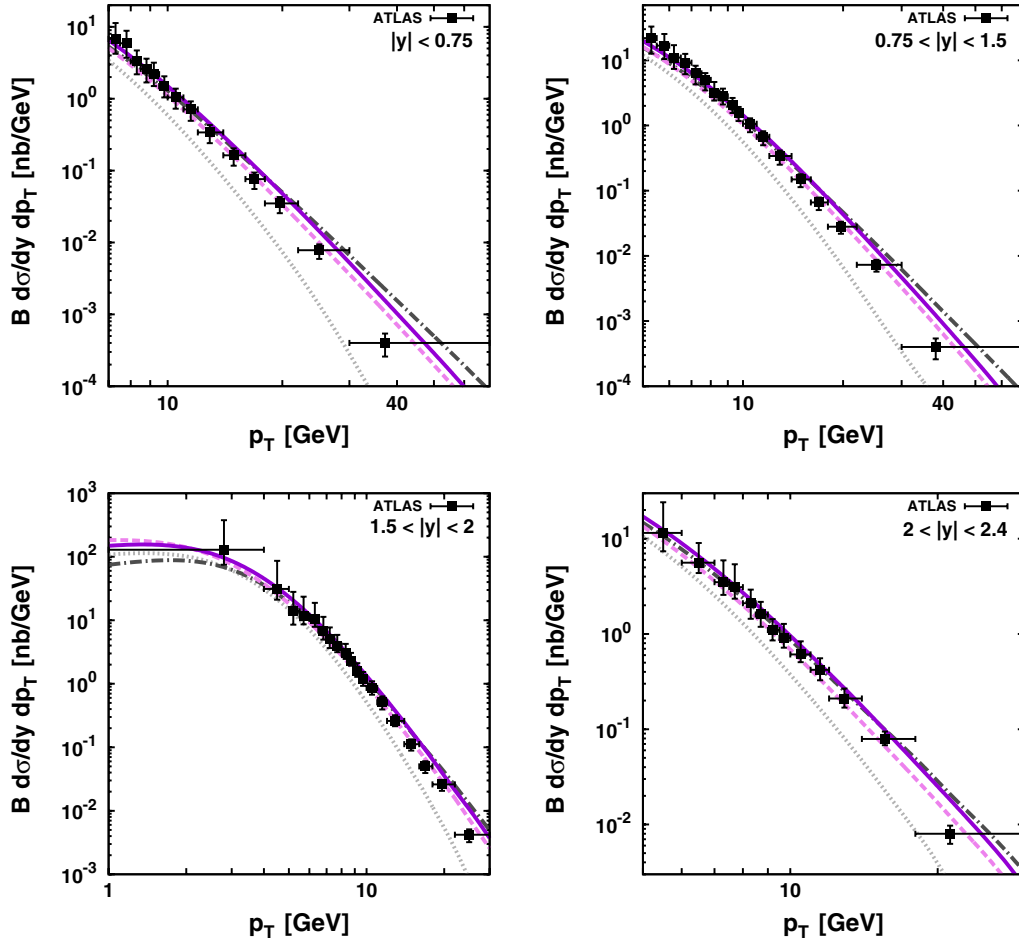


FIG. 2 (color online). The double differential cross sections  $d\sigma/dydp_T$  of prompt  $J/\psi$  production at  $\sqrt{s} = 7$  TeV compared to the ATLAS data [27]. Notation of all histograms is the same as in Fig. 1.

with  $n_f = 4$  quark flavors at  $\Lambda_{\text{QCD}} = 200$  MeV, such that  $\alpha_s(M_Z^2) = 0.1232$ . We take  $|\mathcal{R}_{J/\psi}(0)|^2/4\pi = 0.0876 \text{ GeV}^3$ ,  $|\mathcal{R}'_{\chi}(0)|^2 = 0.075 \text{ GeV}^5$ , and  $|\mathcal{R}_{\psi'}(0)|^2/4\pi = 0.0391 \text{ GeV}^3$ . According to [38], the following branching fractions are used:  $B(\chi_{c1} \rightarrow J/\psi + \gamma) = 0.356$ ,  $B(\chi_{c2} \rightarrow J/\psi + \gamma) = 0.202$ ,  $B(\psi' \rightarrow J/\psi + X) = 0.561$ , and  $B(J/\psi \rightarrow \mu^+ \mu^-) = 0.0593$ .

The results of our calculations are presented in Figs. 1–3 in comparison with the CMS, ATLAS, and LHCb data [27–29]. The solid, dashed, and dash-dotted curves correspond to the results obtained using the CCFM A0, B0, and KMR gluon densities, respectively. Everywhere, we separately show the contribution from the direct production mechanism taken solely (dotted curves). In this case, we apply the CCFM A0 gluon density for illustration. It is clear that sole direct production is not sufficient to describe the LHC data. However, we obtain a good overall agreement of our predictions and the data when summing up the direct and feed-down contributions. The latter is important and production of  $J/\psi$  mesons via radiative decays of  $\chi_{cJ}$  and  $\psi'$  mesons even dominates over the direct contribution at large transverse momenta. The reason can be seen in the

fact that the production of  $\chi_{cJ}$  states refers to much lower values of the final-state invariant mass and therefore effectively probes small  $x$  region, where the gluon distributions are growing up. The  $p_T$  coming from the  $2 \rightarrow 2$  hard subprocess is negligibly small. Taken solely, the relevant matrix element scales as  $1/p_T^8$ , compared to the  $p_T$  coming from the initial gluons that scales as  $1/p_T^4$ . So, to a very good approximation, only the total initial  $k_T$  is important for the final state  $p_T$ . Now, the  $\chi_{cJ}$  is produced in a  $2 \rightarrow 1$  subprocess, while the  $J/\psi$  is produced in a  $2 \rightarrow 2$  subprocess. That means, the  $\chi_{cJ}$  gets the entire transverse momentum of the initial state, while the  $J/\psi$  shares it with the co-produced gluon. The above effect makes the direct  $J/\psi$  spectrum softer than that of the  $\chi_{cJ}$ , in contrast with what could be naively expected.

The dependence of our numerical results on the unintegrated PDFs is rather weak and the CCFM and KMR predictions practically coincide. The difference between them can be observed at small  $p_T$  or at large rapidities probed at the LHCb measurements.

Computations [7] performed in the framework of NRQCD, where CO contributions are taken into account,

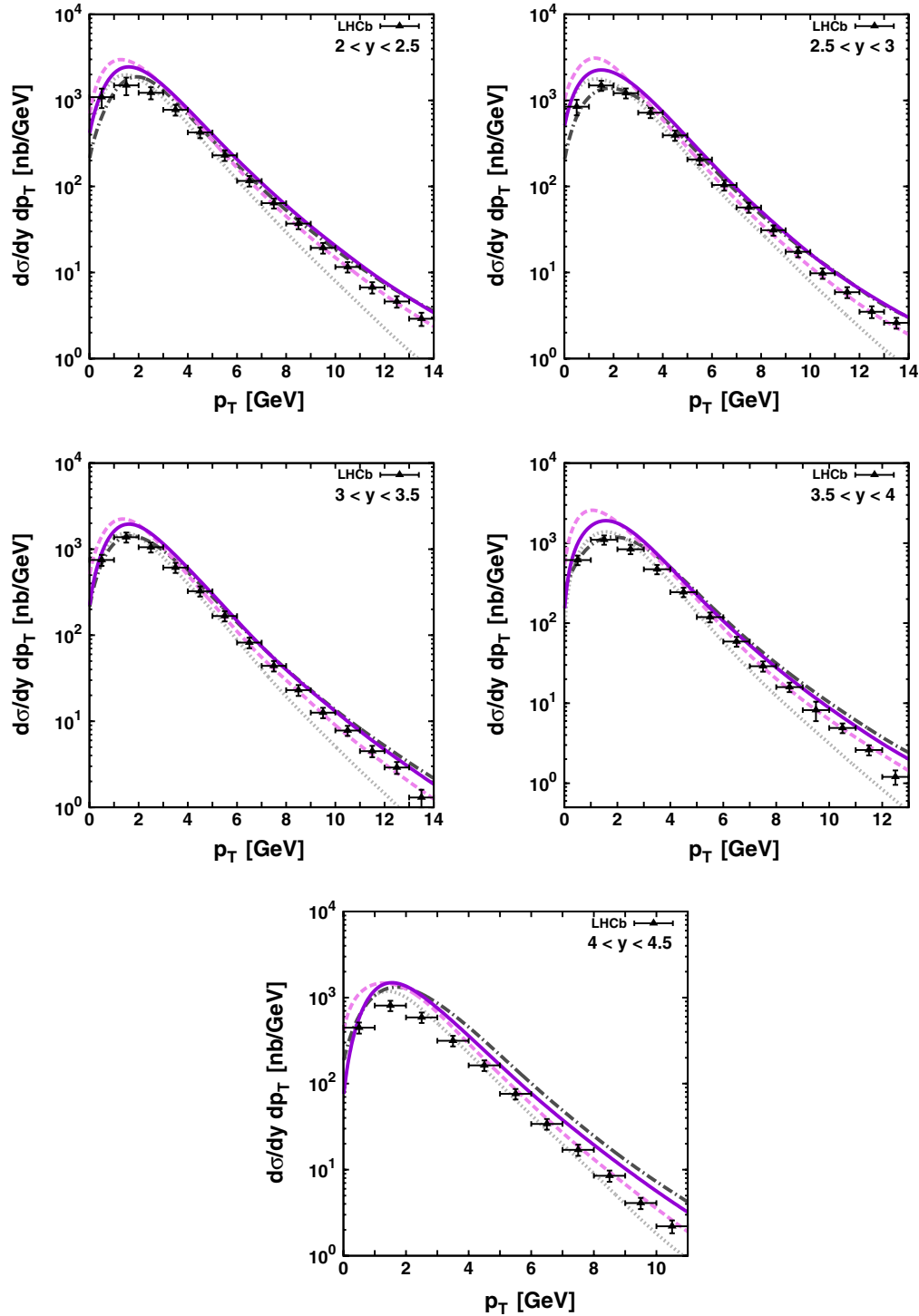


FIG. 3 (color online). The double differential cross sections  $d\sigma/dy dp_T$  of prompt  $J/\psi$  production at  $\sqrt{s} = 7$  TeV compared to the LHCb data [29]. Notation of all histograms is the same as in Fig. 1.

can also explain at satisfactory level the shape and the absolute normalization of the measured  $J/\psi$  cross sections. We find that in the framework of the  $k_T$ -factorization approach there is no need for a CO contribution in the description of  $J/\psi$  production at the LHC. From the other side, the account of high-order

corrections to the CS cross sections calculated in the collinear QCD factorization also leads to the significant improvements in description of the data: the upper bound of the NNLO\* CS predictions is very close [14] to the measurements [27–29] and agree much better (compared to the LO CS results) with the  $k_T$ -factorization

calculations which incorporate a large part of collinear high-order corrections at LO level.

Note that the calculated cross sections of feed-down contributions from the  $P$ -wave states are free from singularities at small transverse momenta. This contrasts with the collinear QCD factorization predictions, which are either unphysical or even divergent.

Now we turn to the  $J/\psi$  polarization. In general, the spin density matrix of a vector particle depends on three parameters  $\lambda_\theta$ ,  $\lambda_\phi$ , and  $\lambda_{\theta\phi}$  which can be measured experimentally. So, the double differential angular distribution of the  $J/\psi \rightarrow \mu^+ \mu^-$  decay products reads [39]

$$\frac{d\sigma}{d\cos\theta^* d\phi^*} \sim 1 + \lambda_\theta \cos^2\theta^* + \lambda_\phi \sin^2\theta^* \cos 2\phi^* + \lambda_{\theta\phi} \sin 2\theta^* \cos\phi^*, \quad (14)$$

where  $\theta^*$  and  $\phi^*$  are the polar and azimuthal angles of the decay lepton measured in the  $J/\psi$  rest frame. Since the polarization parameters  $\lambda_\theta$ ,  $\lambda_\phi$ , and  $\lambda_{\theta\phi}$  (which greatly affects on the cross sections) are not determined yet at the LHC, the results of measurements performed by the CMS, ATLAS, and LHCb collaborations have been presented in a different ways. So, in the ATLAS analysis [27] the unknown  $J/\psi$  polarization has been treated as an additional source of systematic uncertainties. Contrary, the CMS and LHCb collaborations quote their measurements [28,29] for different polarization scenarios: unpolarized ( $\lambda_\theta = 0$ ), full longitudinal polarization ( $\lambda_\theta = -1$ ) and full transverse  $J/\psi$  polarization ( $\lambda_\theta = 1$ ) in the Collins-Soper or the helicity frames.<sup>6</sup> Below we estimate the polarization parameters  $\lambda_\theta$ ,  $\lambda_\phi$  and  $\lambda_{\theta\phi}$  in whole kinematical regions regarding the CMS, ATLAS and LHCb measurements. Our evaluation is generally followed by the experimental procedure. We have collected the simulated events in the kinematical region defined by the CMS, ATLAS and LHCb experiments, generated the decay lepton angular distributions according to the production and decay matrix elements, and then applied a three-parametric fit based on (14). The estimated values of polarization parameters  $\lambda_\theta$ ,  $\lambda_\phi$ , and  $\lambda_{\theta\phi}$  in the helicity (HX) and Collins-Soper (CS) frames are listed in Tables I and II. We find that these parameters are the same in the kinematical regions covered by the CMS and ATLAS collaborations. In order to study the production dynamics in more detail, we separately show contributions from the direct and feed-down mechanisms. The latter, of course, change the polarization of final  $J/\psi$  mesons predicted by the direct production mechanism [21] but this effect is not well pronounced due to overall integration over  $J/\psi$  transverse momentum. Note that the qualitative predictions for the  $J/\psi$  polarization are stable with respect to variations in the model parameters. In fact,

<sup>6</sup>The experimental data points in Figs. 1 and 3 correspond to the unpolarized scenario.

TABLE I. The polarization parameters of prompt  $J/\psi$  mesons calculated in the kinematical region of CMS and ATLAS measurements [27,28]. The CCFM A0 gluon density is used.

Source	$\lambda_\theta$ (HX)	$\lambda_\phi$ (HX)	$\lambda_{\theta\phi}$ (HX)	$\lambda_\theta$ (CS)	$\lambda_\phi$ (CS)	$\lambda_{\theta\phi}$ (CS)
Direct	-0.15	-0.09	0.01	0.20	-0.22	-0.01
Feed-down	0.19	0.14	0.00	0.35	0.09	0.00
Total	-0.07	-0.03	0.01	0.24	-0.14	-0.01

TABLE II. The polarization parameters of prompt  $J/\psi$  mesons calculated in the kinematical region of LHCb measurements [29]. The CCFM A0 gluon density is used.

Source	$\lambda_\theta$ (HX)	$\lambda_\phi$ (HX)	$\lambda_{\theta\phi}$ (HX)	$\lambda_\theta$ (CS)	$\lambda_\phi$ (CS)	$\lambda_{\theta\phi}$ (CS)
Direct	-0.03	-0.13	0.17	0.19	-0.22	-0.03
Feed-down	0.22	0.11	0.13	0.43	0.05	0.05
Total	0.03	-0.07	0.16	0.26	-0.14	-0.01

there is no dependence on the strong coupling constant and unintegrated gluon densities, i.e. two of the important sources of theoretical uncertainties cancel out. Therefore, future precise measurements of the polarization parameters at the LHC will play a crucial role in discriminating the different theoretical approaches.

#### IV. CONCLUSIONS

We have investigated prompt  $J/\psi$  production in  $pp$  collisions at the LHC energy  $\sqrt{s} = 7$  TeV within the framework of the  $k_T$ -factorization approach. Both the direct production mechanism as well as feed-down contributions from  $\chi_{c1}$ ,  $\chi_{c2}$  and  $\psi'$  decays are taken into account. Our consideration is based on the color singlet model supplemented with the off-shell matrix elements for the corresponding partonic subprocesses. The unintegrated gluon densities in a proton are determined using the CCFM evolution equation as well as the Kimber-Martin-Ryskin prescription. We have obtained good agreement of our calculations and the first experimental data taken by the CMS and ATLAS collaborations when summing up the direct and feed-down contributions. The dependence of our predictions on the unintegrated gluon densities appears at small transverse momenta and at large rapidities covered by the LHCb experiment. We have demonstrated also that in the framework of the  $k_T$ -factorization there is no room for a color octet contribution for charmonium production at the LHC.

The estimation of the polarization parameters  $\lambda_\theta$ ,  $\lambda_\phi$ , and  $\lambda_{\theta\phi}$  which determine the  $J/\psi$  spin density matrix is given. The future experimental analysis of the quarkonium polarization at the LHC turned out to be very important and informative for discriminating the different theoretical models.

## ACKNOWLEDGMENTS

We are very grateful to the DESY Directorate for the support in the framework of Moscow—DESY project on Monte-Carlo implementation for HERA—LHC. A. V. L. was supported in part by the grant of the President of Russian Federation (MK-3977.2011.2). Also this research

was supported by the FASI of Russian Federation (Grant No. NS-4142.2010.2), FASI state Contract No. 02.740.11.0244, RFBR Grant No. 11-02-01454-a, and the RMES (grant from the Scientific Research on High Energy Physics).

- 
- [1] M. Krämer, *Prog. Part. Nucl. Phys.* **47**, 141 (2001).
  - [2] J. P. Lansberg, *Int. J. Mod. Phys. A* **21**, 3857 (2006).
  - [3] N. Brambilla *et al.*, *Eur. Phys. J. C* **71**, 1534 (2011).
  - [4] C.-H. Chang, *Nucl. Phys.* **B172**, 425 (1980); E. L. Berger and D. L. Jones, *Phys. Rev. D* **23**, 1521 (1981); R. Baier and R. Rückl, *Phys. Lett. B* **102**, 364 (1981); S. S. Gershtein, A. K. Likhoded, and S. R. Slabospitsky, *Sov. J. Nucl. Phys.* **34**, 128 (1981).
  - [5] E. Braaten and S. Fleming, *Phys. Rev. Lett.* **74**, 3327 (1995).
  - [6] G. Bodwin, E. Braaten, and G. Lepage, *Phys. Rev. D* **51**, 1125 (1995); **55**, 5853 (1997).
  - [7] M. Butenschön and B. A. Kniehl, Report No. DESY 11-046; *Phys. Rev. D* **84**, 051501 (2011).
  - [8] M. Butenschön and B. A. Kniehl, *Phys. Rev. Lett.* **106**, 022003 (2011).
  - [9] Y.-Q. Ma, K. Wang, and K. T. Chao, *Phys. Rev. Lett.* **106**, 042002 (2011).
  - [10] J. Campbell, F. Maltoni, and F. Tramontano, *Phys. Rev. Lett.* **98**, 252002 (2007).
  - [11] P. Artoisenet, J. Campbell, J. P. Lansberg, F. Maltoni, and F. Tramontano, *Phys. Rev. Lett.* **101**, 152001 (2008).
  - [12] J. P. Lansberg, in *Proceedings of Quark Matter 2011* arXiv:1107.0292 ; arXiv:1107.0292.
  - [13] A. Abulencia *et al.* (CDF Collaboration), *Phys. Rev. Lett.* **99**, 132001 (2007).
  - [14] B. Gong and J. X. Wang, *Phys. Rev. Lett.* **100**, 232001 (2008); *Phys. Rev. D* **78**, 074011 (2008).
  - [15] S. P. Baranov, *Phys. Lett. B* **428**, 377 (1998).
  - [16] S. P. Baranov, *Phys. Rev. D* **66**, 114003 (2002).
  - [17] A. V. Lipatov and N. P. Zotov, *Eur. Phys. J. C* **27**, 87 (2003).
  - [18] S. P. Baranov and N. P. Zotov, *J. Phys. G* **29**, 1395 (2003).
  - [19] N. P. Zotov, I. I. Katkov, and A. V. Lipatov, *Phys. At. Nucl.* **69**, 2045 (2006).
  - [20] S. P. Baranov and A. Szczurek, *Phys. Rev. D* **77**, 054016 (2008).
  - [21] S. P. Baranov and N. P. Zotov, *JETP Lett.* **88**, 711 (2008).
  - [22] S. P. Baranov, A. V. Lipatov, and N. P. Zotov, *Eur. Phys. J. C* **71**, 1631 (2011).
  - [23] S. P. Baranov, *Phys. Rev. D* **83**, 034035 (2011).
  - [24] H. Jung, M. Kraemer, A. V. Lipatov, and N. P. Zotov, arXiv:1107.4328.
  - [25] L. V. Gribov, E. M. Levin, and M. G. Ryskin, *Phys. Rep.* **100**, 1 (1983); E. M. Levin, *et al.*, *Sov. J. Nucl. Phys.* **53**, 657 (1991); S. Catani, M. Ciafaloni, and F. Hautmann, *Nucl. Phys.* **B366**, 135 (1991); J. C. Collins and R. K. Ellis, *Nucl. Phys.* **B360**, 3 (1991).
  - [26] B. A. Kniehl, D. V. Vasin, and V. A. Saleev, *Phys. Rev. D* **73**, 074022 (2006).
  - [27] G. Aad *et al.* (ATLAS Collaboration); *Nucl. Phys.* **B850**, 387 (2011).
  - [28] CMS Collaboration, *Eur. Phys. J. C* **71**, 1575 (2011).
  - [29] R. Aaij *et al.* (LHCb Collaboration), *Eur. Phys. J. C* **71**, 1645 (2011).
  - [30] H. Krasemann, *Z. Phys. C* **1**, 189 (1979); G. Guberina, J. Kuhn, R. Peccei, and R. Rückl, *Nucl. Phys.* **B174**, 317 (1980).
  - [31] J. A. M. Vermaseren, Report No. NIKHEF-00-023.
  - [32] P. Cho, M. Wise, and S. Trivedi, *Phys. Rev. D* **51**, R2039 (1995).
  - [33] M. Ambrogiani *et al.* (E835 Collaboration), *Phys. Rev. D* **65**, 052002 (2002).
  - [34] H. Jung, arXiv:hep-ph/0411287.
  - [35] M. A. Kimber, A. D. Martin, and M. G. Ryskin, *Phys. Rev. D* **63**, 114027 (2001); G. Watt, A. D. Martin, and M. G. Ryskin, *Eur. Phys. J. C* **31**, 73 (2003).
  - [36] A. D. Martin, W. J. Stirling, R. S. Thorne, and G. Watt, *Eur. Phys. J. C* **63**, 189 (2009).
  - [37] G. P. Lepage, *J. Comput. Phys.* **27**, 192 (1978).
  - [38] C. Amsler *et al.* (PDG Collaboration), *Phys. Lett. B* **667**, 1 (2008).
  - [39] M. Beneke, M. Krämer, and M. Vanttinen, *Phys. Rev. D* **57**, 4258 (1998).